Electronic Supplementary Material (ESI) for Chemical Communications.

Supporting Information

Porous CoP Nanosheets Converted from Layered Double Hydroxides with Superior Electrochemical Activity for Hydrogen Evolution Reaction at Wide pH Range

YiFan Zeng[1], Yanyong Wang[1], Gen Huang[1], Chen Chen[1], Liangliang Huang[1], Ru Chen[1*],
Shuangyin Wang[1,2,3*]

[1] State Key Laboratory of Chem/Bio-Sensing and Chemometrics, Provincial Hunan Key Laboratory for Graphene Materials and Devices, College of Chemistry and Chemical Engineering, Hunan University, Changsha, 410082, P. R.China.

[2] Key Laboratory of Optoelectronic Devices and Systems of Ministry of Education and Guangdong Province, Shenzhen University, Shenzhen, 518060, P. R.China.

[3] Shenzhen Research Institute of Hunan University, Shenzhen, 518057, P. R.China.

**Corresponding author E-mail: chenru@hnu.edu.cn; shuangyinwang@hnu.edu.cn.*

Experimental section.

Preparation of CoAl-LDH/CP. In a typical procedure, $Co(NO_3)_2 \cdot 6H_2O$ (2 mmol), $Al(NO_3)_3 \cdot 6H_2O$ (2 mmol), NH_4F (8 mmol) and $CO(NH_2)_2$ (10 mmol) were dissolved in 36 mL distilled water and stirred to form a clear solution. The aqueous solution and carbon paper (CP, about 3cm×4cm) were transferred to a 50 mL stainless-steel autoclave, maintained at 100 °C for 24 h, and then allowed to cool to room temperature within 15 min using cooling water. The pink thin film on the CP substrate was immersed in 5 mol L^{-1} (5M) NaOH for 1-3 min and subsequently rinsed with distilled water and ethanol for 5 minutes with the assistance of ultrasonic, and finally dried at 80 °C for 6 h.

Preparation of mesoporous $Co(OH)_2$/CP. Immersing CoAl-LDH/CP in 5 mol·L^{-1} NaOH solution with vigorous agitation for 10 h, rinsed several times by distilled water, and then dried at 80 °C for 6 h.

Preparation of p-CoP/CP. The mesoporous $Co(OH)_2$/CP (1×2 cm) was placed in a porcelain boat and the other porcelain boat containing 0.30 g NaH_2PO_2 was placed at the upstream of the tube furnace. The two alumina boats were calcined at 300 °C for 2 h with a heating speed of 2 °C min^{-1} under N_2 flow and then cooled down to room temperature naturally. Finally, the sample was rinsed several times by distilled water and dried at 80 °C for 6 h.

Electrodeposition of α-$Co(OH)_2$/CP. The electrodeposition was performed in a three electrode cell consisting of carbon paper (2 cm×3 cm) as working electrode, a carbon paper (2 cm×3 cm) as counter electrode and saturated calomel electrode (SCE) as reference electrode at room temperature. The $Co(OH)_2$ was electrodeposited on carbon paper (2 cm×3 cm) in a 0.05 M $Co(NO_3)_2.6H_2O$ aqueous electrolyte. The potential is -1.0 V (vs SCE). After 20 minutes electrodeposition, the green carbon paper was carefully rinsed with deionized water and ethanol and finally dried in air.

Preparation of CoP/CP. The α-$Co(OH)_2$/CP (1×2 cm) was placed in a porcelain boat and the other porcelain boat containing 0.30 g NaH_2PO_2 was placed at the upstream of the tube furnace. The two alumina boats were calcined at 300 °C for 2 h with a heating speed of 2 °C min^{-1} under N_2 flow and then cooled down to room temperature naturally Finally, the sample was rinsed several times by distilled water and dried at 80 °C for 6 h.

Electrochemical Characterization. Electrochemical measurements were performed with CHI 760D electrochemical workstation in a standard three-electrode setup, with the use of p-CoP/CP (p-CoP loading: 5.8 mg cm^{-2}), CoP/CP (CoP loading: 5.4 mg cm^{-2}), Pt/C on CP and pure carbon paper as the working electrode, a graphite rod as the counter electrode and a saturated calomel electrode (SCE) as the reference electrode. Polarization curves were measured using the linear sweeping voltammetry (LSV) method with a scan rate of 5 mV s^{-1} in 0.5 M H_2SO_4 solution (pH=0.6), 1.0 M KOH solution (pH = 13.6), and 1.0 M PBS solution (PH = 7.2) at room temperature. The potential scale with respect to reverse hydrogen electrode (RHE) was adjusted by the Nernst equation, where Evs RHE = $E_{vs\ SCE}$ + 0.0592 × pH + 0.242 (V). The ohmic potential drop (iR) losses from the solution resistance were applied to all initial data according to the following equation: Ecorr = Emea - iR. The potentials reported in this work were expressed versus RHE.

Physical Characterization. The morphology of the samples was investigated by scanning electron microscope (SEM, Hitachi, S-4800) and transmission electron microscope (TEM, FEI Tecnai G20). The crystal structures of the samples were characterized using powder X-ray diffraction (XRD, Bruker D8 Advance diffractometer, Cu Kα1). The nitrogen adsorption-desorption isotherms were measured at 77 K with a Quantachrom NOVA 1000e system.

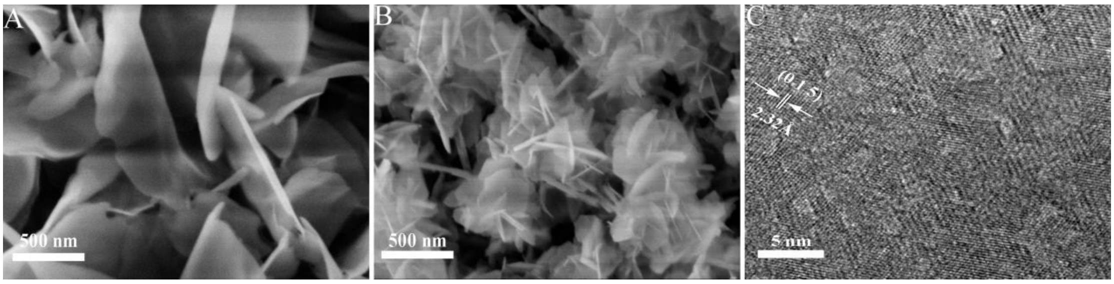

Figure S1. Typical SEM images of (A) CoAl-LDH (B) SEM images of mesoporous $Co(OH)_2$ (C) HRTEM image of mesoporous $Co(OH)_2$.

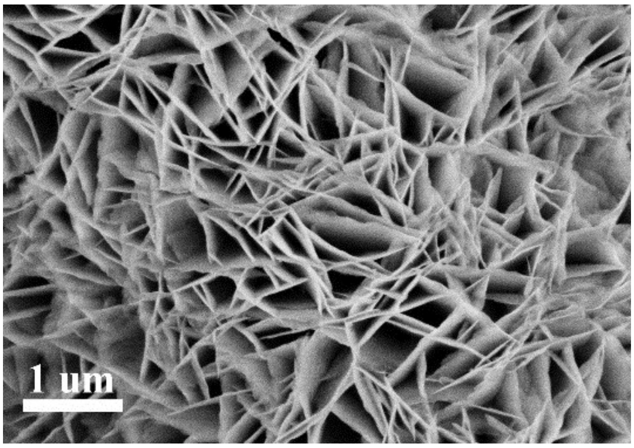

Figure S2. Typical SEM images of α-$Co(OH)_2$.

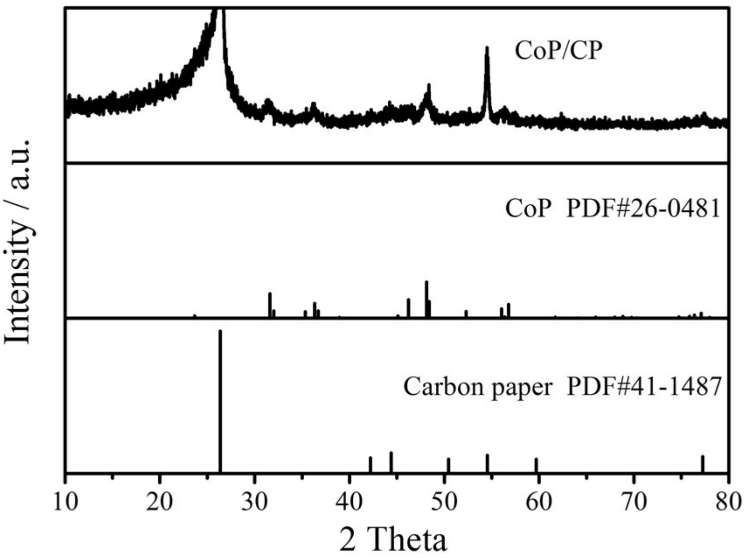

Figure S3. XRD pattern of CoP/CP.

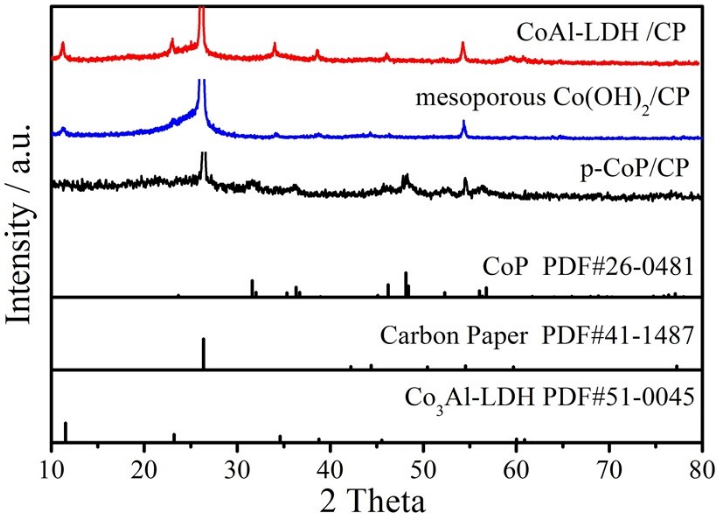

Figure S4. XRD pattern of CoAl-LDH/CP, mesoporous $Co(OH)_2$/CP, and p-CoP/CP.

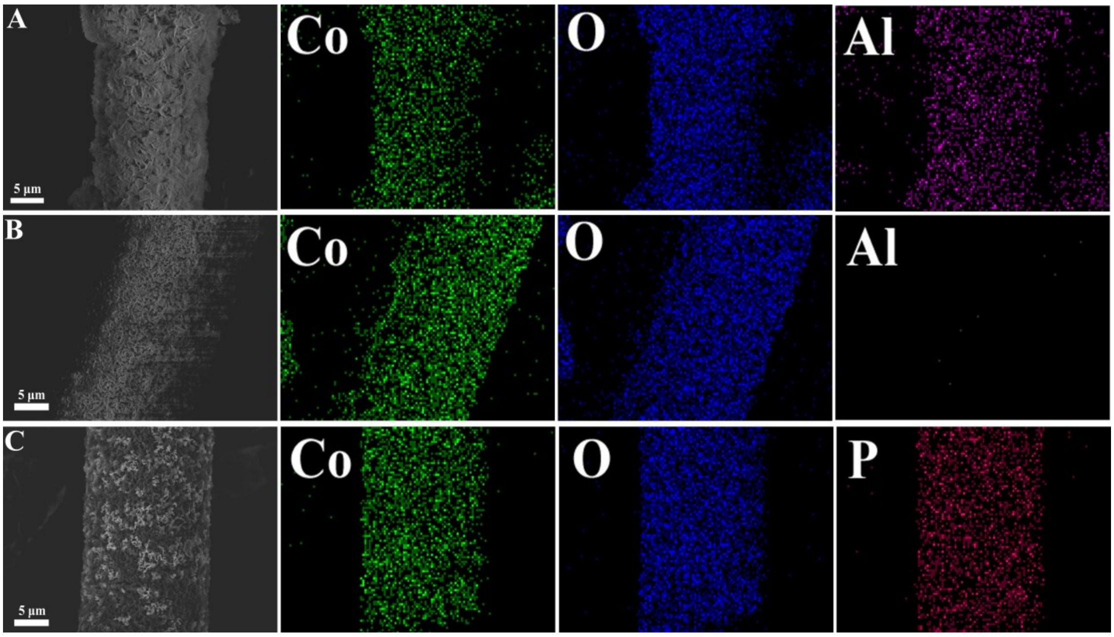

Figure S5. SEM image and EDX elemental mapping of (A) CoAl-LDH/CP (B) mesoporous $Co(OH)_2$/CP and (C) p-CoP/CP.

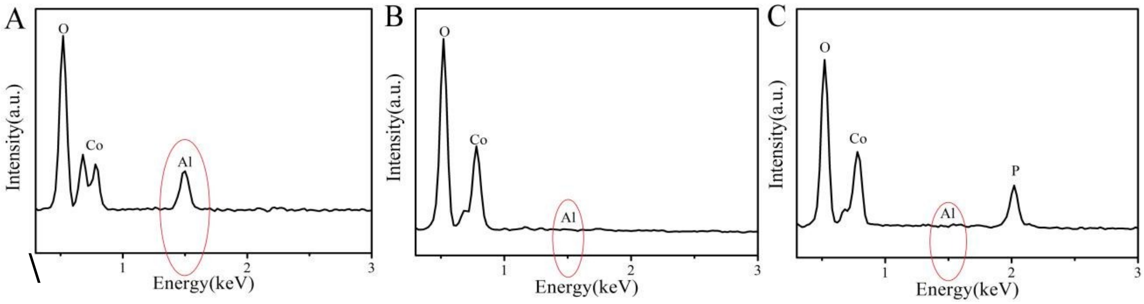

Figure S6. The EDX spectrums of (A) CoAl-LDH (B) mesoporous $Co(OH)_2$ and (C) p-CoP.

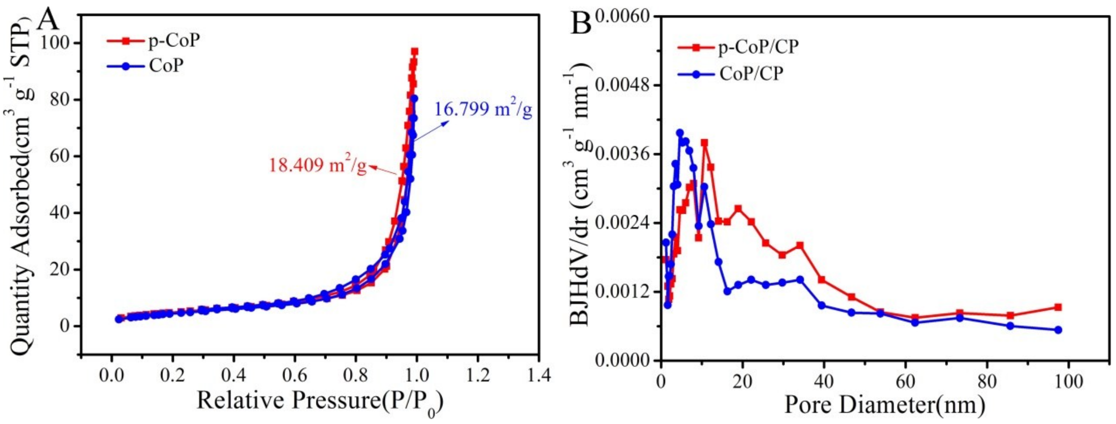

Figure S7. (A) N_2 adsorption-desorption isotherms of CoP and p-CoP (B) Corresponding BJH pore size distribution.

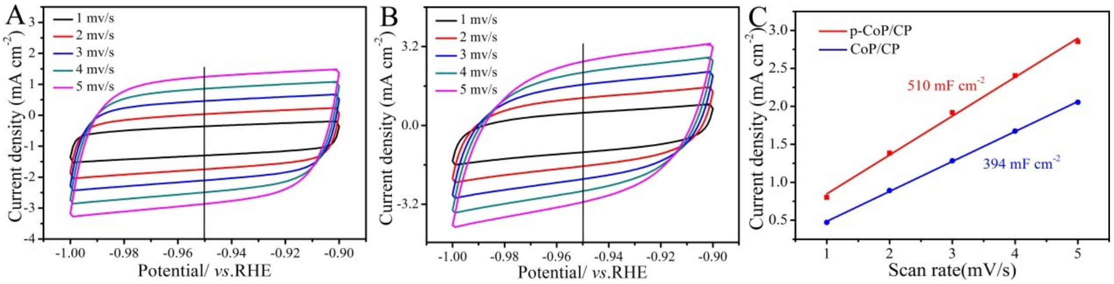

Figure S8. Tested the electrochemical surface area (ECSA) of CoP/CP and p-CoP/CP in 1.0 M KOH solution. (A) Cyclic voltammetry curves of CoP/CP and (B) p-CoP/CP with different scanning rates. The capacitive current measured at -0.95 V vs RHE was plotting as a function of scan rate (C) CoP/CP and p-CoP/CP.

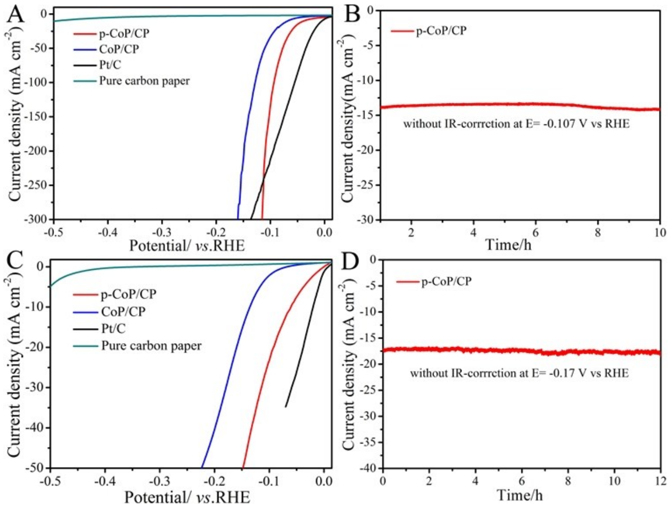

Figure S9. (A) Polarization curves recorded for p-CoP/CP, CoP/CP, Pt/C, Pure carbon paper with a scan rate of 5 mV s^{-1} for HER and (B) Time-dependent current density curves of p-CoP at an E = -0.107 V vs RHE in 0.5 M H_2SO_4 (C) Polarization curves recorded for p-CoP/CP, CoP/CP, Pt/C, Pure carbon paper with a scan rate of 5 mV s^{-1} for HER and (D) Time-dependent current density curves of p-CoP at an E= -0.17 V vs RHE in 1.0 M PBS.

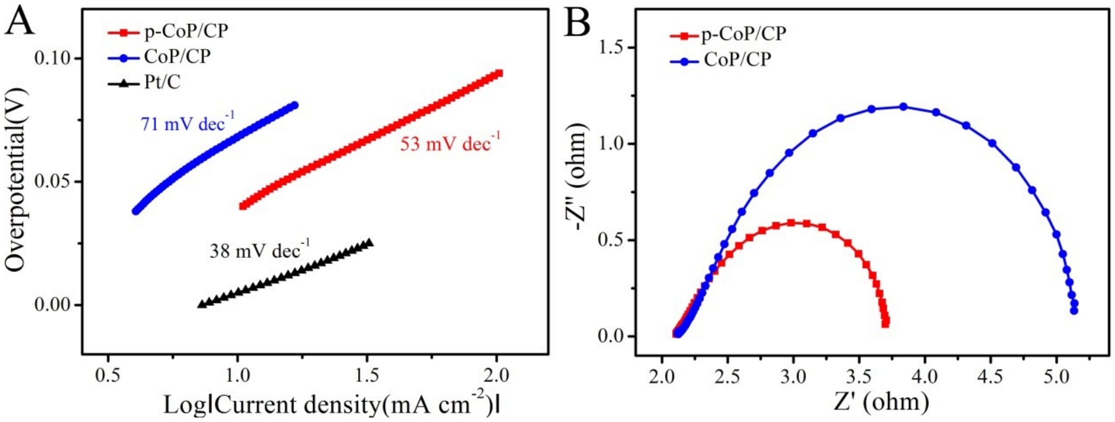

Figure S10. (A) Tafel plots of p-CoP/CP，CoP/CP , Pt/C in 0.5 M H_2SO_4 and (B) Nyquist plots of p-CoP/CP, CoP/CP at -80 mV vs RHE.

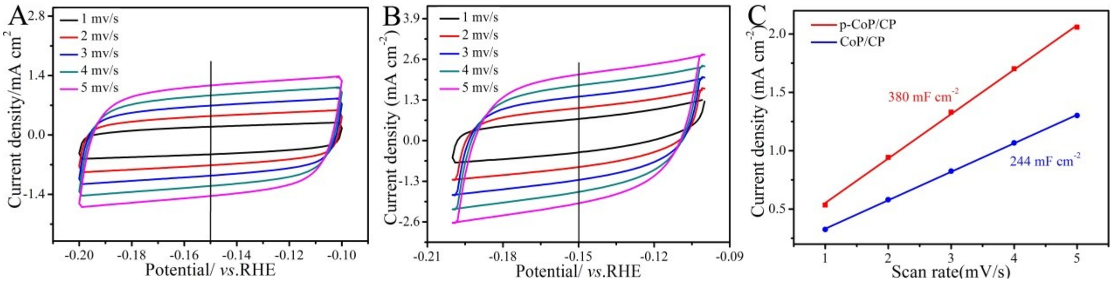

Figure S11. Tested the electrochemical surface area (ECSA) of CoP/CP and p-CoP/CP in 0.5 M H_2SO_4 solution. (A) Cyclic voltammetry curves of CoP/CP and (B) p-CoP/CP with different scanning rates. The capacitive current measured at -0.15 V vs RHE was plotting as a function of scan rate (C) CoP/CP and p-CoP/CP.

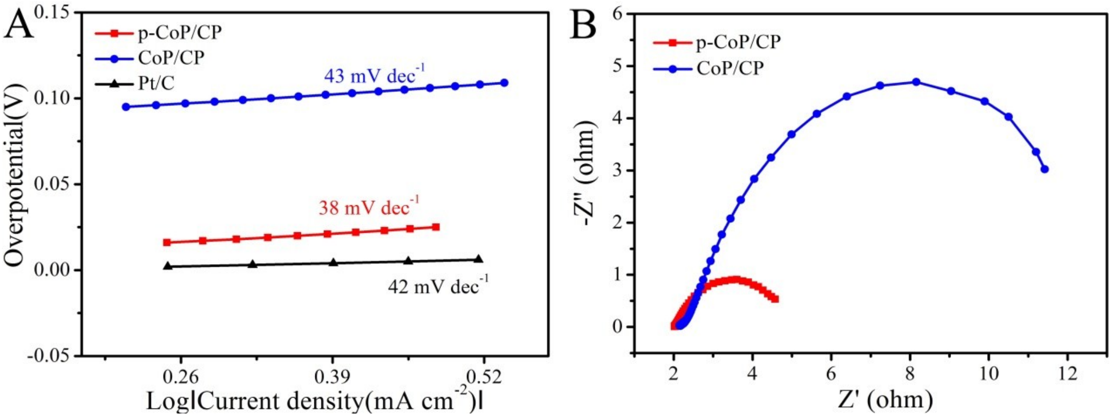

Figure S12. (A) Tafel plots of p-CoP/CP, CoP/CP, Pt/C in 1.0 M PBS and (B) Nyquist plots of p-CoP/CP, CoP/CP at -119 mV vs RHE in 1.0 M PBS.

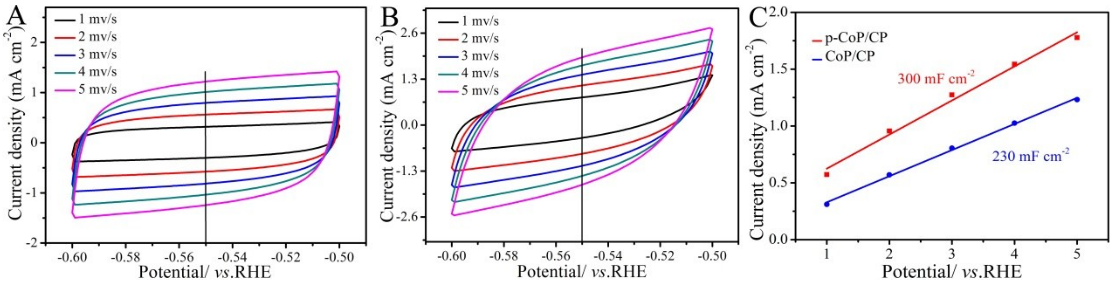

Figure S13. Tested the electrochemical surface area (ECSA) of CoP/CP and p-CoP/CP in 1.0 M PBS solution. (A) Cyclic voltammetry curves of CoP/CP and (B) p-CoP/CP with different scanning rates. The capacitive current measured at -0.55 V vs RHE was plotting as a function of scan rate (C) CoP/CP and p-CoP/CP.

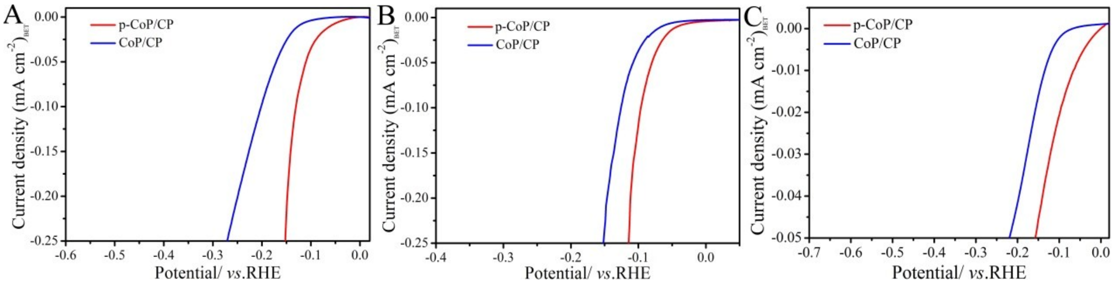

Figure S14. The HER performance of the CoP/CP, p-CoP/CP after BET normalization in different electrolytes (A) 1.0 M KOH (B) 0.5 M H_2SO_4 and (C) 1.0 M PBS.

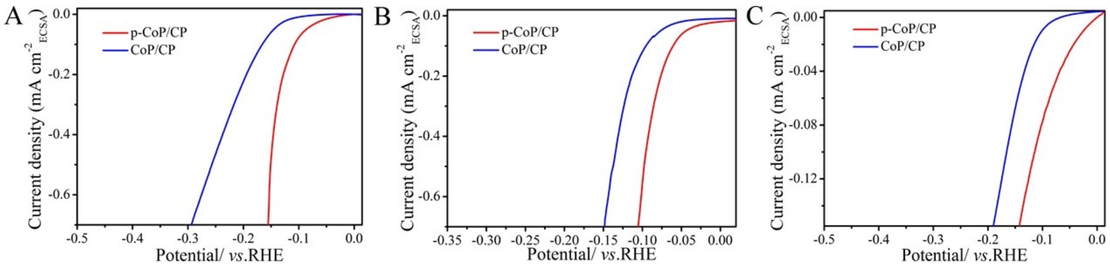

Figure S15. The HER performance for CoP/CP and p-CoP/CP after normalization of the electrochemical active area (A) 1.0 M KOH (B) 0.5 M H_2SO_4 and (C) 1.0 M PBS.

Table S1. The element analysis of the CoAl-LDH, mesoporous $Co(OH)_2$ and p-CoP.

Materials	Co (atom percentage content, %)	Al (atom percentage content, %)	P (atom percentage content, %)	The element mole ratio of Co/Al	The element mole ratio of Co/P
CoAl-LDH	13.06	12.48	-	1.05	-
Mesoporous $Co(OH)_2$	29.72	-	-	-	-
p-CoP	22.32	-	19.21	-	1.16

Table S2. Comparison of HER performance for p-CoP/CP with other CoP-related materials in 1.0 M KOH.

Electrocatalyst	Electrolyte solution	Current density (mA cm^{-2})	Overpotential at the corresponding Current density (mV)	Reference
p-CoP/CP	1M KOH	10	57	This work
CoP/CP	1M KOH	10	128	
Mn−Co−P/Ti	1M KOH	10	76	[1]
$Zn_{0.08}Co_{0.92}P$/TM	1M KOH	10	67	[2]
CoP/TM	1M KOH	10	99	
u−CoP/Ti	1M KOH	10	60	[3]
CoP nanoneedles on carbon cloth fibers	1M KOH	10	95	[4]
Fe-CoP/Ti	1M KOH	10	78	[5]
CoP_2/RGO	1M KOH	10	88	[6]
Ce-doped CoP/Ti	1M KOH	10	92	[7]
Ni–Co–P–300	1M KOH	10	150	[8]
CoP_3 NAs/CFP	1M KOH	10	119	[9]
CoP NS/C	1M KOH	10	111	[10]

Table S3. Comparison of HER performance for p-CoP/CP with other CoP-related materials in 0.5 M H_2SO_4.

Electrocatalyst	Electrolyte solution	Current density (mA cm^{-2})	Overpotential at the corresponding Current density (mV)	Reference
p-CoP/CP	0.5M H_2SO_4	10	38	This work
CoP/CP	0.5M H_2SO_4	10	69	
CoP nanowire/CC	0.5M H_2SO_4	10	67	[11]
CoP_2/RGO	0.5M H_2SO_4	10	70	[6]
CoP/Ti	0.5M H_2SO_4	10	~75	[12]
np-CoP NWs/Ti	0.5M H_2SO_4	10	78	[13]
CoP NA/Ti	0.5M H_2SO_4	10	90	[14]
$Fe_{0.5}Co_{0.5}P$	0.5M H_2SO_4	10	130	[15]
$Zn_{0.08}Co_{0.92}P$/TM	0.5M H_2SO_4	10	39	[2]
CoP/TM	0.5M H_2SO_4	10	82	
Co_2P nanorods	0.5M H_2SO_4	10	134	[16]
CoP/rGO	0.5M H_2SO_4	10	105	[17]
CoP nanosheets	0.5M H_2SO_4	10	56	[18]

Table S4. Comparison of HER performance for p-CoP/CP with other non-noble-metal HER electrocatalysts in 1.0 M PBS.

Electrocatalyst	Electrolyte solution	Current density (mA cm^{-2})	Overpotential at the corresponding Current density (mV)	Reference
p-CoP/CP	1.0M PBS	10	60	This work
CoP/CP	1.0M PBS	10	136	
CoP nanowire/CC	1.0M PBS	10	106	[11]
Mn-Co-P/Ti	1.0M PBS	10	86	[1]
np-CoP NWs/Ti	1.0M PBS	10	178	[13]
CoP NA /Ti	0.2M PBS	10	149	[14]
MoP2 NS/CC	1.0M PBS	10	85	[19]
NiS2/CC	1.0M PBS	10	243	[20]
Ni3S2/Ni foam	1.0M PBS	10	170	[21]
MoS2/Ti plate	1.0M PBS	10	200	[22]
Co9S8/CC	1.0M PBS	10	175	[23]
WP/CC	1.0M PBS	10	200	[24]

References:

1. T. Liu, X. Ma, D. Liu, S. Hao, G. Du, Y. Ma, A. M. Asiri, X. Sun and L. Chen, Acs Catalysis, 2017, 7.
2. T. Liu, D. Liu, F. Qu, D. Wang, L. Zhang, R. Ge, S. Hao, Y. Ma, G. Du and A. M. Asiri, Advanced Energy Materials, 2017, 7, 1700020.
3. D. Zhou, L. He, W. Zhu, X. Hou, K. Wang, G. Du, C. Zheng, X. Sun and A. M. Asiri, Journal of Materials Chemistry A, 2016, 4.
4. P. Wang, F. Song, R. Amal, Y. H. Ng and X. Hu, Chemsuschem, 2016, 9, 472.
5. C. Tang, R. Zhang, W. Lu, L. He, X. Jiang, A. M. Asiri and X. Sun, Advanced Materials, 2017, 29.
6. J. Wang, W. Yang and J. Liu, Journal of Materials Chemistry A, 2016, 4, 4686-4690.
7. W. Gao, M. Yan, H. Y. Cheung, Z. Xia, X. Zhou, Y. Qin, C. Y. Wong, J. C. Ho, C. R. Chang and Y. Qu, Nano Energy, 2017.
8. Y. Feng, X.-Y. Yu and U. Paik, Chemical Communications, 2016, 52, 1633-1636.
9. T. Wu, M. Pi, D. Zhang and S. Chen, Journal of Materials Chemistry A, 2016, 4, 14539-14544.
10. J. Chang, L. Liang, C. Li, M. Wang, J. Ge, C. Liu and W. Xing, Green Chemistry, 2016, 18, 2287-2295.
11. J. Tian, Q. Liu, A. M. Asiri and X. Sun, Journal of the American Chemical Society, 2014, 136, 7587-7590.
12. E. J. Popczun, C. G. Read, C. W. Roske, N. S. Lewis and R. E. Schaak, Angewandte Chemie, 2014, 126, 5531-5534.
13. S. Gu, H. Du, A. M. Asiri, X. Sun and C. M. Li, Physical Chemistry Chemical Physics, 2014, 16, 16909.
14. Z. Pu, Q. Liu, P. Jiang, A. M. Asiri, A. Y. Obaid and X. Sun, Chemistry of Materials, 2014, 26, 4326-4329.
15. J. Kibsgaard, C. Tsai, K. Chan, J. D. Benck, J. K. Nørskov, F. Abild-Pedersen and T. F. Jaramillo, Energy & Environmental Science, 2015, 8, 3022-3029.
16. Z. Huang, Z. Chen, Z. Chen, C. Lv, M. G. Humphrey and C. Zhang, Nano Energy, 2014, 9, 373-382.
17. L. Jiao, Y.-X. Zhou and H.-L. Jiang, Chemical Science, 2016, 7, 1690-1695.
18. C. Zhang, Y. Huang, Y. Yu, J. Zhang, S. Zhuo and B. Zhang, Chemical Science, 2017, 8, 2769-2775.
19. W. Zhu, C. Tang, D. Liu, J. Wang, A. M. Asiri and X. Sun, Journal of Materials Chemistry A, 2016, 4, 7169-7173.
20. C. Tang, Z. Pu, Q. Liu, A. M. Asiri and X. Sun, Electrochimica Acta, 2015, 153, 508-514.
21. L.-L. Feng, G. Yu, Y. Wu, G.-D. Li, H. Li, Y. Sun, T. Asefa, W. Chen and X. Zou, J. Am. Chem. Soc, 2015, 137, 14023-14026.
22. J. Shi and J. Hu, Electrochimica Acta, 2015, 168, 256-260.
23. L.-L. Feng, M. Fan, Y. Wu, Y. Liu, G.-D. Li, H. Chen, W. Chen, D. Wang and X. Zou, Journal of Materials Chemistry A, 2016, 4, 6860-6867.
24. Z. Pu, Q. Liu, A. M. Asiri and X. Sun, ACS applied materials & interfaces, 2014, 6, 21874-21879.